THE ASTROPHYSICAL JOURNAL, 225:919–931, 1978 November 1

COORDINATED ULTRAVIOLET, OPTICAL, AND RADIO OBSERVATIONS OF HR 1099 AND UX ARIETIS

E. J. WEILER
Princeton University Observatory
F. N. OWEN*
National Radio Astronomy Observatory,† Green Bank, West Virginia
B. W. BOPP* AND M. SCHMITZ
Ritter Observatory, The University of Toledo
D. S. HALL*
Dyer Observatory, Vanderbilt University
DOROTHY A. FRAQUELLI
David Dunlap Observatory, University of Toronto
V. PIIROLA
Observatory and Astrophysics Laboratory, University of Helsinki
M. RYLE
Cavendish Laboratory, Madingley Road, Cambridge, England
AND
D. M. GIBSON
Nuffield Radio Astronomy Laboratories, Jodrell Bank, Macclesfield, Cheshire, England
Received 1978 January 3; accepted 1978 May 11

ABSTRACT

Simultaneous radio, visual, and ultraviolet observations of the RS Canum Venaticorum binaries UX Arietis and HR 1099 are reported. The joint program covered the interval 1976 September 22 through October 3. The observations consisted of (1) radio flux density measurements at 1660, 2695, and 8085 MHz; (2) UV spectrophotometry of Lα and Mg II *h* and *k*; (3) Hα and Ca II H and K spectroscopy; (4) *V*-band photometry; and (5) *UBV* polarimetry.

As in many of the RS Canum Venaticorum binaries, a quasi-sinusoidal variation in *V* was observed in both systems. The period of this variation was approximately equal to the orbital period. No significant optical polarization was observed from either system. Variable radio emission was detected from both binaries throughout the program.

Variable Hα and Lα emission were observed from HR 1099. UX Ari also exhibited Lα emission. Multiple Mg II emission components with peculiar velocities of up to 250 km s^{-1} were often seen from both systems. Each Mg II observation also exhibited a strong and variable central velocity component which always seemed to match the orbital velocity of the more massive star in each system. HR 1099 exhibited strong Ca II H and K emission which was not significantly variable.

The joint observations provide strong evidence for chromospheric activity associated with the more massive star in each binary. Although the radio emission is produced in a larger volume than the optical and UV activity, temporal correlations suggest that a physical connection may exist between the two phenomena.

Subject headings: stars: eclipsing binaries — stars: individual — stars: radio radiation — ultraviolet: spectra

I. INTRODUCTION

The stars HR 1099[1] (G5–K0 IV + G5 V) and UX Arietis (G5 V + K0 IV) are two of the brightest RS Canum Venaticorum–type binaries, a class defined by Hall (1976). Both systems show marked spectroscopic and photometric peculiarities. Variable emission is present at both the Ca II H and K lines and Hα (Weiler 1978*a*; Bopp and Fekel 1976), and periodic low-amplitude variations in *V* are sometimes seen (Hall 1977; Bopp *et al.* 1977). These phenomena are usually associated with the cooler or subgiant components in RS Canum Venaticorum systems. Perhaps the outstanding peculiarity of both binaries is the

* Guest Investigator with the Princeton University telescope on the *Copernicus* satellite, which is sponsored and operated by the National Aeronautics and Space Administration.

† Operated by Associated Universities, Inc., under contract with the National Science Foundation.

[1] V711 Tauri.

presence of variable radio emission at centimeter wavelengths. HR 1099 and UX Ari are usually observed at flux densities of ~30 mJy at a frequency of 8085 MHz, but radio flares which increase the flux density by an order of magnitude have been observed (Gibson, Hjellming, and Owen 1975; Owen, Jones, and Gibson 1976; Spangler, Owen, and Hulse 1977). A variety of arguments (Hall 1976) link the observed optical peculiarities with a model for the RS Canum Venaticorum binaries incorporating intense stellar surface activity, notably in the form of star spots. The origin of the radio emission is less clear. Although the emission probably arises in a larger circumstellar volume (see Owen, Jones, and Gibson 1976; Owen and Spangler 1977), it may be associated in some way with the stellar surface phenomena.

In order to search for correlations among the various observed phenomena, we have carried out a coordinated program of observations of HR 1099 and UX Ari at ultraviolet, optical, and radio wavelengths during the interval 1976 September 22–October 3. In most cases, all ground-based observations during the joint campaign were coordinated with the *Copernicus* program of three 1 day intervals on UX Ari separated by two 3 day intervals on HR 1099. The following observational techniques were employed: (1) radio observations at 1660, 2695, and 8085 MHz (Gibson, Owen, and Ryle); (2) *Copernicus* observations of Mg II *h* and *k* (λ2800) and Lα (Weiler); (3) Spectroscopic observations of the Ca II H and K and Hα emission lines (Bopp, Fraquelli, and Schmitz); (4) *V*-band photometry (Hall); and (5) *UBV* polarimetry (Piirola). During the interval of the observations, strong radio flares were observed from both systems. Variable Hα emission was also observed from HR 1099. In the UV, both binaries displayed strong Mg II emission lines with variable profiles. Both systems also exhibited broad Lα emission. This paper describes these observations and suggests a possible relation among the UV, optical, and radio phenomena.

II. GROUND-BASED PHOTOMETRY

In late 1976 and early 1977, 66 differential observations of UX Ari and 96 of HR 1099 were obtained photoelectrically in *V* at four different observatories. These are described in detail by Landis *et al.* (1978). Plotted in Figures 1 and 2 are nightly normals of the Δ*V* magnitudes obtained at each observatory or normals of three observations if as many as six were made in one night at one observatory. A quasi-sinusoidal distortion wave, often seen in RS Canum Venaticorum binaries (Hall 1976), is clearly present in both figures.

The comparison star for UX Ari was 62 Ari. Phases in Figure 1 are computed with the ephemeris

$$\text{JD(hel.)} = 2{,}440{,}133.76 + 6^{d}.43791\ E \qquad (1)$$

for which the period is the spectroscopically determined orbital period (Carlos and Popper 1971) and zero phase corresponds to conjunction with the cooler (more active) star in front.

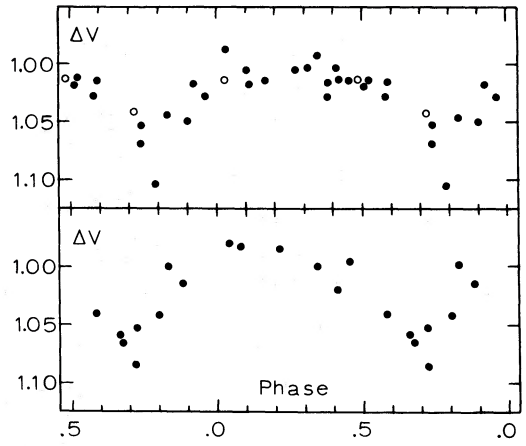

FIG. 1.—Light curve of UX Ari. Open circles are normals of observations made within the time span of the *Copernicus* observations. The upper part (JD 2,442,990.8 through 2,443,117.8) shows that wave minimum occurred around phase 0.8 in late 1976. The lower part (JD 2,443,129.6 through 2,443,211.6) shows minimum around phase 0.7 in early 1977.

Examination of the two parts of Figure 1 indicates the light curve of UX Ari may have changed between late 1976 and early 1977. While wave minimum apparently occurred around phase 0.8 in late 1976, it appears to have migrated to phase 0.7 in early 1977. Comparing this photometry with the 1974 photometry, Landis *et al.* (1978) derived a migration period of 8 years but pointed out that the migration rate may have been accelerating. The observations made within the time span of the *Copernicus* observations appear in Figure 1 as open circles; they are consistent with the other 1976 observations.

The comparison star for HR 1099 was 10 Tau. Phases in Figure 2 are computed with the ephemeris

$$\text{JD(hel.)} = 2{,}442{,}766.069 + 2^{d}.83782\ E \qquad (2)$$

for which the period is the spectroscopically determined orbital period (Bopp and Fekel 1976) and zero phase corresponds to conjunction with the more active (the

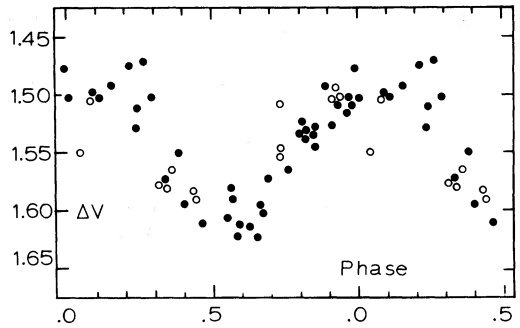

FIG. 2.—Light curve of HR 1099. Open circles are normals of observations made within the time span of the *Copernicus* observations. Wave minimum, taken as the midpoint between the falling and rising branches at $\Delta V = 1.55$ mag, occurred around phase 0.55. The possible flarelike brightening discussed in the text occurred around phase 0.72.

more massive) component in front. Since the more active component in most RS Canum Venaticorum binaries is the cooler component, this conjunction is presumably the one at which primary eclipse would occur if HR 1099 were an eclipsing binary. The ephemeris of Bopp and Fekel (1976) had zero phase at periastron; the ephemeris of Bopp *et al.* (1977) had zero phase at minimum light as of 1976.0. All orbital phases quoted for both binaries in this paper are computed with the two ephemerides in equations (1) and (2).

Taking the midpoint between the falling and rising branches at $\Delta V = 1.55$ mag in Figure 2, we see that the wave minimum occurs at phase 0.55 ± 0.01 as of 1977.0. On the basis of this and earlier photometry, Landis *et al.* (1978) derived a mean migration period of 13 ± 1 years.

The observations made within the time span of the *Copernicus* observations appear in Figure 2 as open circles. With the exception of two nights, they are consistent with the other 1976–1977 observations. The eight individual observations obtained at two of the observatories between October 3 0615 and 0726 UT (around phase 0.72) show HR 1099 to have brightened from $\Delta V = 1.55$ mag to $\Delta V = 1.40$ mag. This may indicate a flarelike event, but unfortunately most of the increase was observed at only one of the observatories and hence cannot be confirmed. The observation on October 1 (around phase 0.04) appears about 0.05 mag fainter than other observations at the same phase, but unfortunately HR 1099 was observed on this night at only one observatory.

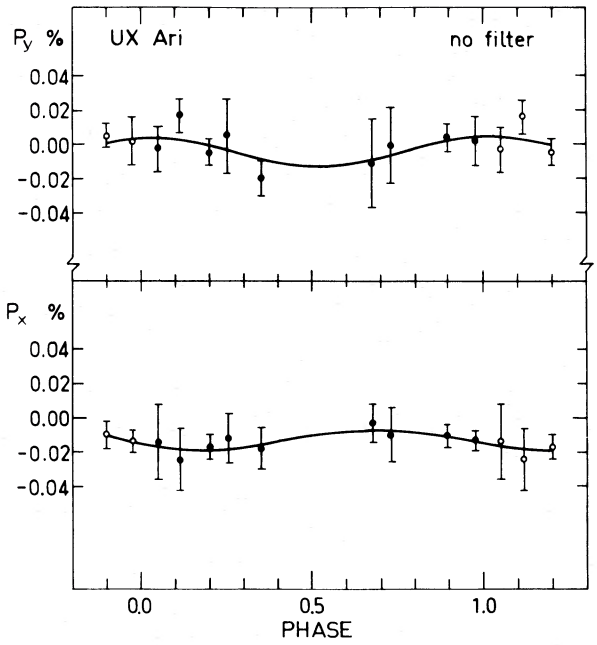

FIG. 3.—Nightly averages of the polarization parameters $P_x = P \cos 2\theta$ and $P_y = P \sin 2\theta$ plotted as a function of orbital phase for UX Ari. The error bars correspond to the standard errors of the mean values. The smooth curves are the fundamental Fourier components.

III. POLARIMETRY

Following the suggestion of Dr. R. H. Koch, polarization observations of UX Ari and HR 1099 were made at the Metsähovi Observatory of the University of Helsinki during the interval 1976 September 21 to October 2. The dual beam-chopping polarimeter described by Piirola (1973, 1975) was used with a 60 cm Ritchey-Chrétien telescope. UX Ari was observed on nine nights and HR 1099 on five nights. The low declination of HR 1099 ($+0°31'$) and the high latitude of the observatory ($+60°$) limited the usable observing time for HR 1099 to about 2 hours during each night.

Both binaries were observed without filters; UX Ari was also observed with standard *UBV* filters. The photomultiplier was an EMI 6256 SA. With 40 s effective integration time at each of the eight position angles of the instrument and one 10 s integration for the sky, the time for one complete observation was about 12 minutes. Sky background polarization was directly and optically eliminated by using a plane-parallel calcite plate as the polarizing beam splitter (Piirola 1973, 1975). Instrumental polarization has been found to be very small and stable ($\pm 0.003\%$) as determined by observations of unpolarized nearby stars.

In Figures 3 and 4 the nightly averages of the normalized Stokes parameters $P_x = P \cos 2\theta$ and

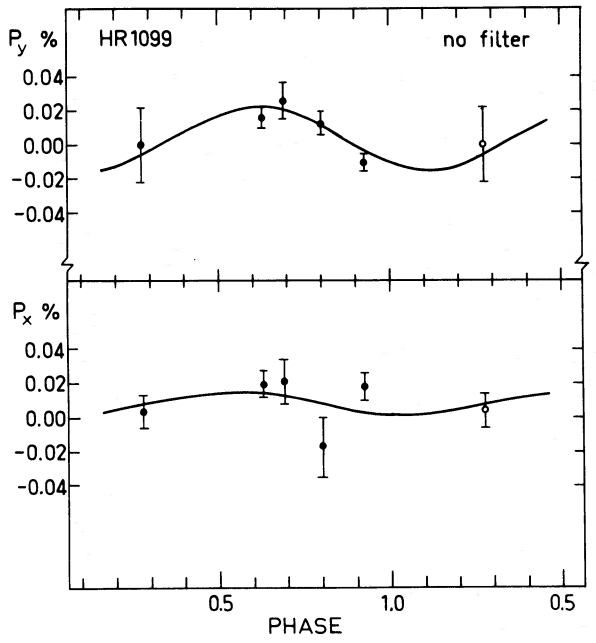

FIG. 4.—Nightly averages of the polarization parameters $P_x = P \cos 2\theta$ and $P_y = P \sin 2\theta$ plotted as a function of orbital phase for HR 1099. The error bars correspond to the standard errors of the mean values. The smooth curves are the fundamental Fourier components.

$P_y = P \sin 2\theta$ are plotted as a function of orbital phase. The error bars correspond to the standard errors of the mean values. The smooth curves are the fundamental Fourier components. These components for HR 1099 may have physical significance, since the wavelike distortions in the light curves are quasi-sinusoidal and the maximum polarization occurs near photometric wave minimum. However, amplitudes of the polarization variations are small and could be accounted for by statistical noise in the data.

Table 1 gives the overall mean values of the polarization parameters, $\langle P_x \rangle$ and $\langle P_y \rangle$, with their standard errors, standard deviations of individual observations, σ_x and σ_y, direct mean values of the internal standard errors, $\langle \epsilon_{\rm int} \rangle$, and the number of observations, n. The internal standard error of each observation is computed from the measurements made in the eight position angles of the polarimeter. The average polarizations are very small for both UX Ari and HR 1099. The standard deviations (rms scatters) of P_x and P_y are in no case significantly larger than the averages of the internal errors. Accordingly, the scatter of the individual observations could be explained as being due to random errors, mainly photon noise. Also the larger errors in the U are due to photon noise, as the signal in U was about 10% of that in B and V for UX Ari.

IV. RADIO OBSERVATIONS

Radio observations of HR 1099 and UX Ari were made (1) at 2695 and 8085 MHz with the Green Bank interferometer, (2) at 2695 MHz with the Cambridge 5 km telescope, and (3) at 1660 MHz with the Jodrell Bank Mark I–Mark II interferometer. The results of the Green Bank and Cambridge observations were also part of continuing programs which are described in more detail elsewhere (Owen and Gibson 1978; Hine and Ryle 1978).

Of particular interest is the large flare observed on September 24 from HR 1099 after the star had been unusually weak at 2695 and 8085 MHz (Fig. 5). This event appears to coincide in time with the peak Hα and Lα activity observed during this program and discussed in §§ V and VI. Unlike the large flare of 1976 March 10–12 (Owen *et al.*), the spectrum of this event steepened as it decayed. On September 24 $\alpha_{2695}^{8085} = 0.49 \pm 0.12$, while on September 25 $\alpha_{2695}^{8085} = -0.43 \pm 0.12$ ($S \propto \nu^{\alpha}$). At the peak of the flare, a limit of less than 5% can be placed on the degree of circular polarization at both frequencies. However, on September 25, HR 1099 was between 10% and 20% left-hand circularly polarized at 2695 MHz. The star may also have been marginally right-hand circularly polarized ($\sim 10\%$) at 8085 MHz, especially between 0500 and 0800 UT. During the remaining days, HR 1099 was not especially strong and on September 29 had dropped down close to its minimum of September 23.

UX Ari remained relatively inactive in the September 24–29 interval except for a relatively strong event on September 27–28 UT. On October 2, an unusual, rapidly brightening flare was observed at 1660 MHz which rose from 28 ± 8 mJy at 0300 UT to 73 ± 8 mJy at 0310 UT and 63 ± 8 mJy at 0320 UT.

V. Ca II H AND K AND Hα SPECTROSCOPY

HR 1099 is a double-line spectroscopic binary (SB2), with absorption lines from both components having approximately equal intensity (Bopp and Fekel 1976). There are very strong emission features at Ca II H and K which share the velocity of the more massive (and more active) component, and much weaker features at the velocity of the second star. In the red, Hα is seen in emission and seems to follow the velocity of the more active star (Bopp and Fekel 1976). The Hα emission is variable in equivalent width (EW), and profile variations are visible at moderate (1 Å) resolution.

Spectroscopic observations of the Hα and Ca II H and K emission lines of HR 1099 were made at Ritter Observatory and David Dunlap Observatory (DDO) during the campaign. (UX Ari observations were clouded out at both sites.) At Ritter Observatory, a total of 27 image-tube spectrograms of the Hα region were obtained with the 1 m reflector and Cassegrain spectrograph. The spectra were recorded on nitrogen-baked 127-04 emulsion, at a dispersion of 40 Å mm^{-1} and resolution of 1.2 Å. Exposure times were 15–20 minutes. Reduction of the data was conventional, using the Ritter microphotometer; EW measurements of Hα were made graphically, with internal single spectrogram errors of $\sim 10\%$–20%.

The eight spectrograms obtained on September 24 UT, when the radio flux density was strongly enhanced, show a mean Hα emission equivalent width $\langle \rm EW \rangle \sim 1.1$ Å, stronger than the emission observed several months earlier ($\langle \rm EW \rangle \sim 0.7$ Å) by Bopp and Fekel. The EW apparently decreased with time. On

TABLE 1

POLARIZATION PARAMETERS FOR UX ARIETIS AND HR 1099

Star (1)	Filter (2)	$\langle P_x \rangle$% (3)	σ_x% (4)	$\langle P_y \rangle$% (5)	σ_y% (6)	$\langle \epsilon_{\rm int}$% $\rangle$ (7)	n (8)
UX Ari.....	None	−0.014 ± 0.004	0.032	0.002 ± 0.004	0.032	0.032	58
UX Ari.....	*V*	−0.016 ± 0.006	0.031	0.004 ± 0.008	0.038	0.035	25
UX Ari.....	*B*	−0.003 ± 0.009	0.043	0.002 ± 0.011	0.050	0.035	22
UX Ari.....	*U*	−0.002 ± 0.018	0.082	0.021 ± 0.018	0.079	0.084	20
HR 1099....	None	+0.015 ± 0.005	0.025	0.011 ± 0.005	0.024	0.032	25

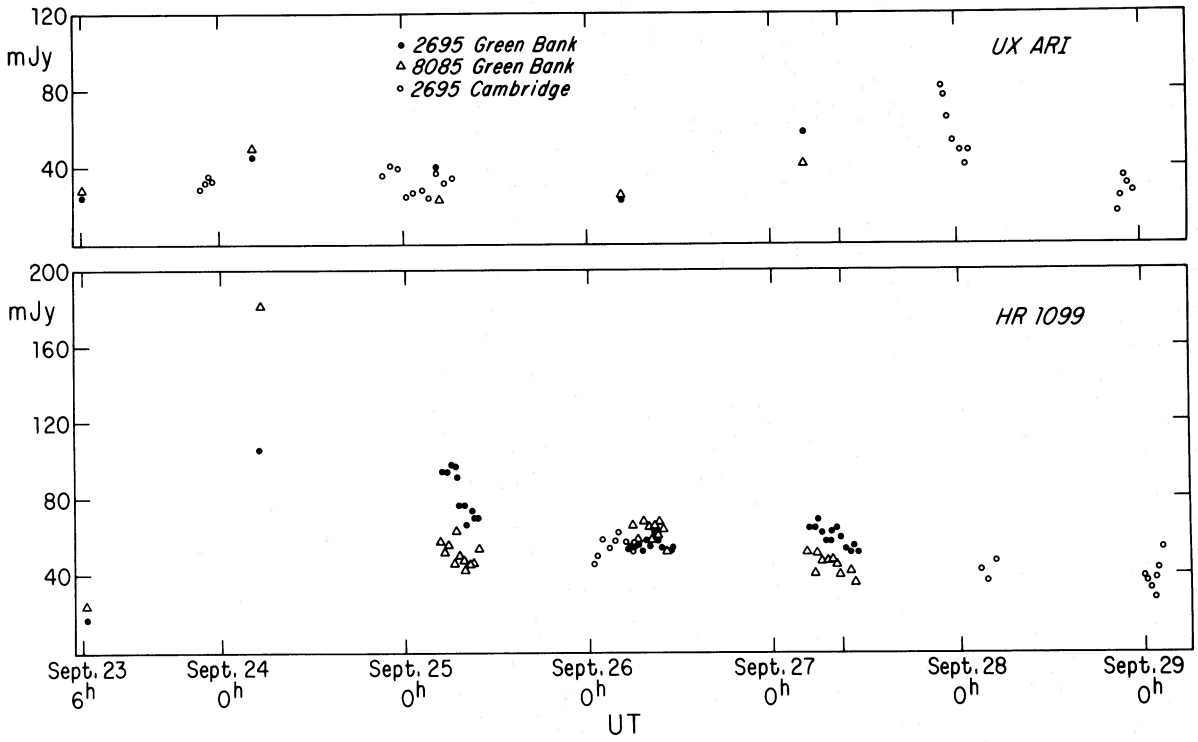

FIG. 5.—Radio flux densities for HR 1099 and UX Ari during the campaign. *Open circles*, from the Cambridge 5 km telescope at 2695 MHz; *filled circles*, from the Green Bank interferometer at 2695 MHz; *triangles*, from the Green Bank interferometer at 8085 MHz. One standard deviation for all observed points is at most ~10% of the observed value.

September 25 and 29 UT, $\langle EW \rangle \sim 0.7$ Å, and by October 1 UT it had declined to ~0.4 Å (Fig. 6).

The Ritter EW measurements on September 24 UT, and perhaps on September 25 UT and 29 UT also, show a scatter that is greater than normal. We believe this represents a real, rapid variation in EW, and is not simply the result of random error. The scatter is *not* always present in Hα EW data. On 1977 February 8, a similar series of Hα observations of HR 1099 were obtained, and reduced in identical fashion. Six spectrograms with ~20 minute time resolution yielded $\langle EW \rangle = 0.71 \pm 0.03$ Å (standard deviation of a single measure). This may be compared with $\langle EW \rangle = 1.08 \pm 0.27$ Å obtained on September 24 UT. Furthermore, the Ritter data show a definite bimodal distribution in EW on September 24, tending to have values

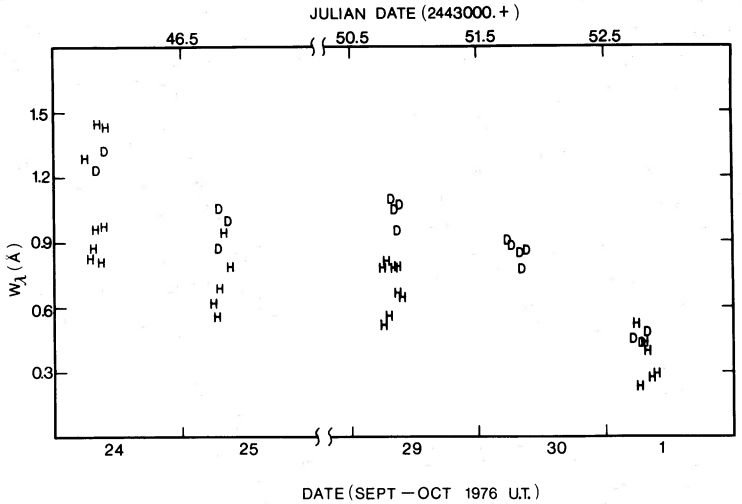

FIG. 6.—The Hα emission equivalent widths plotted against UT (*lower axis*) and Julian date (*upper axis*) for HR 1099. The H's are the Ritter Observatory data and the D's those of DDO. The combined data show a general decrease in equivalent width with time. Note that on September 24 UT, after a strong radio outburst, the Ritter data show rapid variations in equivalent width.

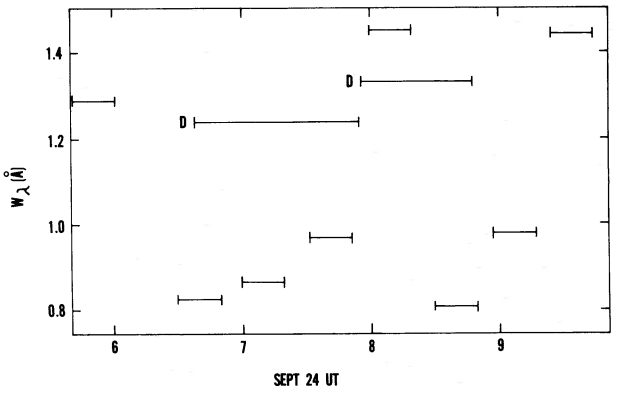

FIG. 7.—The Hα equivalent widths plotted against time for September 24 UT for HR 1099. The D's to the right of a given line indicated DDO data. The others are Ritter data. The high time resolution Ritter spectrograms show marked EW variations.

near either 1.4 Å or 0.9 Å; such a distribution is not the result of random scatter (Fig. 7).

At DDO spectrograms of the Hα and Ca II H and K regions were obtained with the 1.88 m reflector during approximately the same time interval. Seventeen red spectra were recorded on vacuum-sensitized 098-01 emulsion at a dispersion of 16 Å mm^{-1} and 11 blue spectra obtained with IIa-O plates at 12 Å mm^{-1}. Rectified intensity tracings of the DDO plate material were produced by using the DDO microdensitometer system. The data were noise-filtered with a 24 μm (FWHM) Gaussian truncated at 3 σ. The red plates were calibrated with the local version of the Latham spot sensitometer (Latham 1969). The internal error of the DDO Hα EW measurements is on the order of 10%. The blue plates were calibrated by exposing a density step tablet in contact with the plate to diffuse illumination. All calibrations were developed at the same time as the spectrograms.

The Hα EW measurements from the DDO spectrograms show pronounced variations with time. The general behavior follows that of the Ritter data, with a maximum EW on September 24 UT, followed by a decline to minimum EW (~0.5 Å) on October 1 UT (Fig. 6). The Ritter data appear to have systematically smaller EWs than the DDO data. This effect is probably a result of the different techniques used to determine continuum levels and the differing spectral resolutions. The DDO EW measurements include the contribution from low-level emission in the wings which was not detectable in the lower-resolution Ritter data. No convincing evidence for variations in Hα EW are seen on the September 24 UT DDO data, but exposure times for the DDO red plates were ~45 minutes, so variations on a shorter time scale might have been missed. (We note that when the temporal resolution of the Ritter data is degraded to that of the DDO measures, then no rapid EW changes are noticeable.)

The higher resolution afforded by the DDO spectrograms allows the Hα and Ca II H and K profiles to be examined for multiple features. The Hα emission has a total width approximately twice that of the stellar absorption lines and shows noticeable variations in profile; much of this variability may be linked with orbital phase. Figure 8 shows the line profiles at four different orbital phases. The broad, flat emission seen near phase 0.016 is similar to the broad profiles reported by Bopp and Fekel (at a similar phase) and Wilson (1964). The major peak in the Hα emission profiles occurs at the velocity of the more active component. Other peaks are also seen in the profiles, one of which appears to follow the velocity of the less active star. The data, however, are poorly distributed in phase, so that this behavior requires confirmation. The superposition of telluric water-vapor absorption lines has been ruled out as a possible source of the emission peaks.

Equivalent-width measurements in the Ca II H and K region were complicated by the double-line nature of HR 1099. This region has a high density of lines in the single-line phase, and when the lines double, it becomes nearly impossible to define a continuum. The spectrograms were rectified by choosing two stable points in the intensity spectra (λλ3851.2, 4042.1), drawing a straight line between these points, and normalizing the spectrum to this line. We find no evidence for Ca II intensity variations in either star; variable emission is seen to the red of Ca II H, which is probably Balmer Hε associated with a more active component.

Figure 9 shows three calcium profiles at different

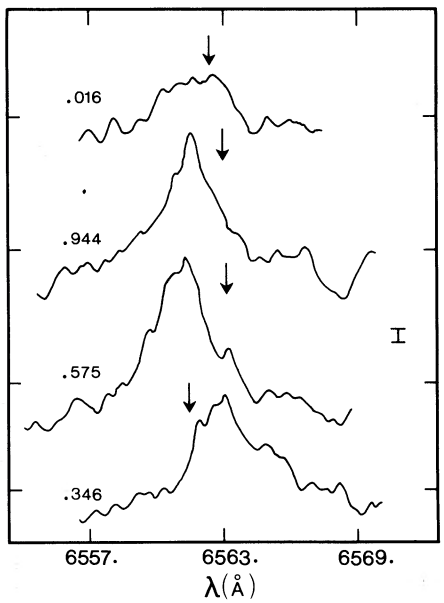

FIG. 8.—Hα emission-line profiles of HR 1099 from the DDO plates. The numbers to the left of each profile refer to the orbital phase, and the fiducial marks represent the continuum level for each profile. The bar represents 5% of continuum. The arrows give the expected position of emission from the less active component.

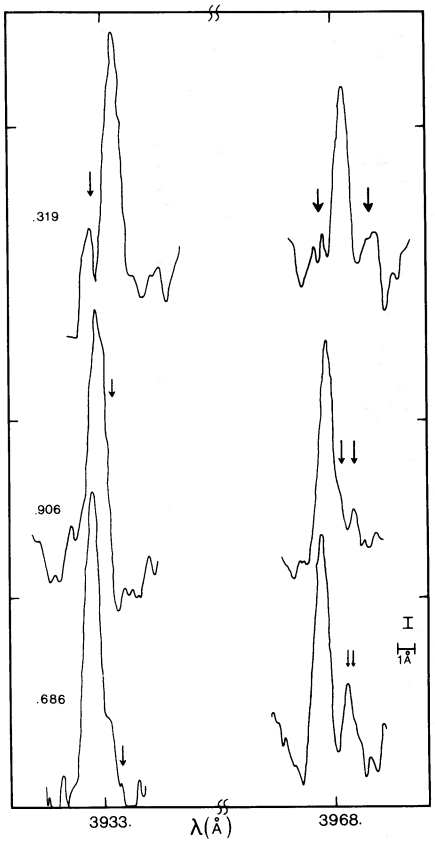

FIG. 9.—Ca II H and K line profiles of HR 1099 from the DDO plates. The numbers to the left of each profile set refer to orbital phase, and the fiducial marks represent the continuum level. The bars represent 5% of continuum and 1 Å, respectively. The arrows give the positions of the secondary emission components and the Hε λ3970 emission line.

orbital phases. At phase 0.319, both the H and K lines show blueshifted components from the less active star; emission to the red of the Ca II H line is Balmer Hε from the more active star. At phase 0.906, the Ca II emission from the two stars is blended, and a weak Hε emission component is seen. At phase 0.686, the velocities of Ca II H in the less active star and Hε in the more active star nearly overlap, but the virtual invisibility of the Ca II K line in the less active component argues that most of this strong feature to the red of the Ca II H line is due to Hε emission.

VI. ULTRAVIOLET OBSERVATIONS

Princeton's ultraviolet spectrometer aboard the *Copernicus* satellite (Rogerson *et al.* 1973) was used to obtain high-resolution scans of Lα and the Mg II *h* and *k* doublet at λ2800 from HR 1099 and UX Ari. Both binaries displayed measurable emission which varied in intensity over time scales of less than a day. The mere detection of UV emission in these two systems is significant, as both are 2–3 mag fainter than the faintest, single, late-type stars observed with *Copernicus* which have exhibited chromospheric Lα and Mg II emission (Anderson 1977, private communication). In this section we will present several of the line scans and the major results of the UV observations. For a more detailed discussion of the observations, including special background subtraction techniques, see Weiler (1978*b*).

a) Lα *Observations*

Each photoelectric spectrum scan covered 2.9 Å centered at λ1215.65 with a resolution of 0.05 Å. To reduce noise, four sequential scans were combined over intervals of 5–7 hours. In all, 21 such composite observations of HR 1099 were obtained and the total line strength was found to vary by a factor of about 2. Although the profiles were very broad (>2.5 Å), they did seem to reflect the orbital velocity of the more active star.

Figure 10 is a plot of Lα emission strength (integrated line intensity) of HR 1099 versus time. The 2 σ error bar at the upper right represents an estimated error which is due mainly to uncertainty in determining a continuum level. No detectable continuum is expected from faint late-type stars at Lα or Mg II with *Copernicus*. Thus, all the signal seen in the UV is due to line emission. The arrows along the abscissa represent photometric wave minima and tend to correlate with times of stronger emission.

Another noteworthy feature of Figure 10 is the particularly strong Lα emission observed at 1200 UT on September 24 immediately following the intense radio flare. Since there was only one radio observation of this flare at 0500 UT, it is impossible to determine whether the radio outburst had peaked at that time or was still increasing. Hα emission remained exceptionally strong up to the conclusion of these observations at 0830 UT.

Figure 11*a* is the corresponding, composite Lα line scan. The 2 σ error bar is the Poisson error, and the small arrow indicates the velocity of the more active star. Adjacent channels were averaged to reduce

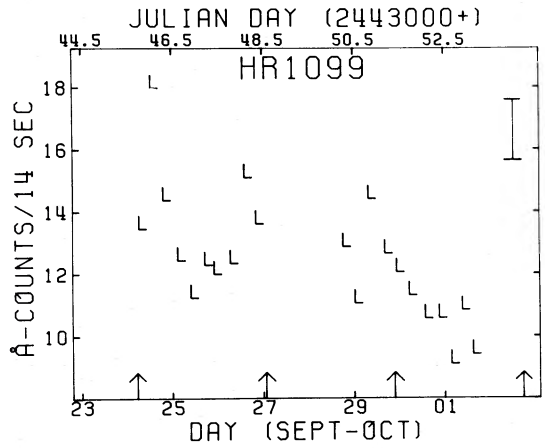

FIG. 10.—HR 1099 Lα emission intensity versus civil and Julian date. Arrows along the abscissa represent successive photometric wave minima. The error bar is ±1 σ.

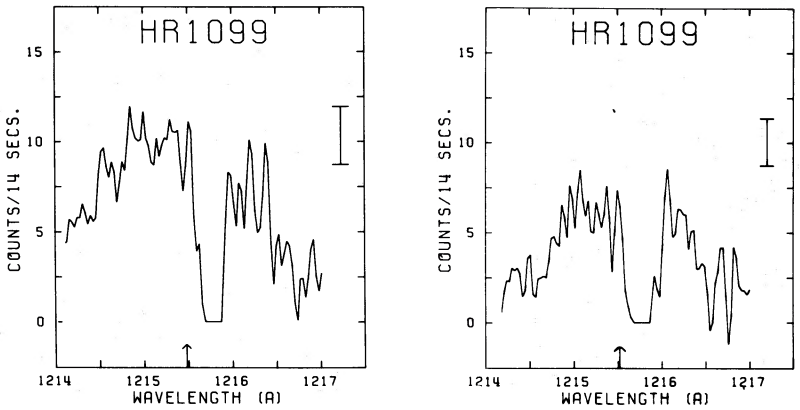

FIG. 11.—(*a*) Composite Lα line scan of HR 1099 obtained over a 6 hr interval and centered at 1200 UT on September 24. The small arrow on the abscissa represents the rest frame of the more active star. The central depression is due to interstellar H I absorption. The error bar is ±1 σ. The orbital phase is 0.68. (*b*) Composite Lα line scan of HR 1099 obtained over a 7 hr interval and centered at 2100 UT on September 30. The error bar is ±1 σ. Orbital phase is 0.91.

noise and thus the effective resolution of this and subsequent Lα profiles is only 0.1 Å. The profile is very broad and probably does not include the entire breadth of the greatly enhanced blue wing. The large central depression is due mainly to interstellar absorption (Anderson and Weiler 1978), while the flat portion of the profile in this depression represents the channels from which the geocoronal contamination was removed. For comparison, Figure 11*b* is typical of a composite scan in which the line strength was low.

Twelve composite Lα observations of UX Ari were also obtained during three separate 1 day observing runs (September 23 and 28 and October 2). The composite line scans were very noisy because the signal was less than one-half that of the HR 1099 data. An emission strength analysis was conducted, but any potential systematic variations were lost in the overall noise of the data. The mean emission strength level on the night of October 2 UT (the same night as the unusual 1660 MHz radio flare) was slightly higher, but even this result was well within the expected observational error and cannot be considered significant.

b) Mg II *Observations*

Each scan covered effectively 4 Å centered at Mg II *k* λ2795.5 or Mg II *h* λ2802.7 at a resolution of 0.51 Å. In each 6 hour interval 30 to 40 such scans were collected, but only those scans obtained in the least noisy segments of each orbit were actually used to produce composite line profiles (Weiler 1978*b*). A total of 18 composite Mg II *k* and six Mg II *h* scans from HR 1099 were collected, while 12 *k* line scans of UX Ari were obtained.

The total Mg II line strength apparently varied randomly by a factor of 2 in both systems. This analysis was complicated greatly by the frequent presence of multiple emission features as well as the noisy nature of *Copernicus* near-UV data. One of these emission features matched closely the velocity of the more active star in each system, while one or two features were sometimes observed at velocities

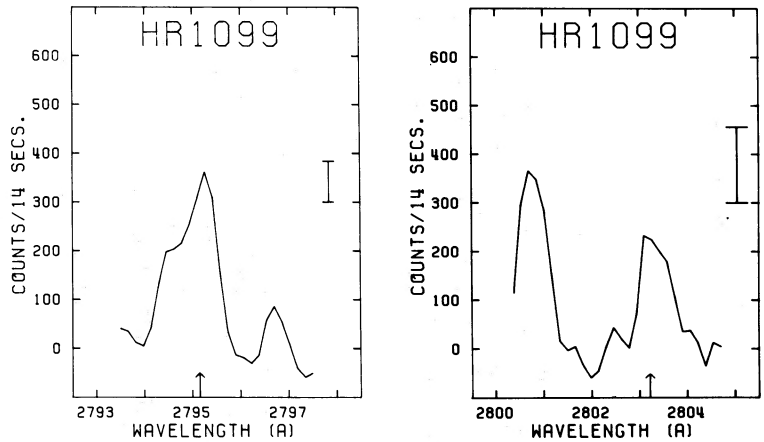

FIG. 12.—(*a*) Composite Mg II *k* line scan of HR 1099 obtained over a 6 hr interval and centered at 1300 UT on September 24. The small arrow on the abscissa represents the rest frame of the more active star on this and subsequent figures. The error bar is ±1 σ. Orbital phase is 0.69. (*b*) Composite Mg II *h* line scan of HR 1099 obtained over a 4 hr interval and centered at 0300 UT on September 29. Note the significantly displaced feature around 2801 Å. The error bar is ±1 σ. Orbital phase is 0.30.

of up to ± 250 km s^{-1} with apparent lifetimes at the same velocity of up to 12 hours. Figure 12*a* is a composite of 34 Mg II *k* scans of HR 1099. This series of scans was obtained after the strong radio outburst of September 24 UT, i.e., during the same interval as the Lα profile displayed in Figure 11*a*. This profile represents one of the few Mg II observations which exhibited only a strong zero-velocity component (with respect to the more active star). The 2 σ error bar in Figure 12*a* and subsequent Mg II profiles was determined by extensive background fluctuation measurements during the actual orbits of observation. The small arrow on this and subsequent profiles represents the velocity of the more active (more massive) star.

Figure 12*b* presents 17 stacked scans of HR 1099's Mg II *h* line obtained on September 29 at 0300 UT. Once again, one feature matches the velocity of the more active star, but another strong feature (5 σ) appears shifted 240 km s^{-1} toward shorter wavelengths. Division of the 17 scans into three roughly equal subsets indicated this feature was present throughout the entire observing period, however. The lifetime of this feature was less than 4 hours, as it did not appear in previous or subsequent observations. Its strength was the greatest of any displaced emission line observed throughout the campaign. This feature followed closely a period of time when the Cambridge radio observations showed HR 1099 to be rapidly brightening (Fig. 5).

UX Ari also exhibited multiple velocity features, as evidenced in Figure 13*a*. This figure is a composite of 22 scans of Mg II *k* centered at 0300 UT on October 2. The velocity of one of the emission features correlates with the orbital velocity of the more active star, while the only other really significant feature is blueshifted 200 km s^{-1}. This emission feature was the strongest displaced component observed in UX Ari and occurred at the same time as the unusually abrupt radio outburst observed at 1660 MHz. Figure 13*b* represents an example of one of the UX Ari composite observations which displayed only a strong central feature.

c) Ultraviolet Emission Luminosity

Table 2 lists the range of the Lα and Mg II line luminosities observed in this study. The Mg II entries refer to line luminosities calculated for the zero-velocity emission features of the more active star in both binary systems. All entries were calculated by using system distances of 33 pc for HR 1099 (Bopp and Fekel 1976) and 50 pc for UX Ari (Hall 1976), and Princeton spectrometer efficiencies as determined by Snow and Torres (1977). The absolute efficiency of the spectrometer is not well known, and the calibration factor at Lα is accurate to 20%, while that at Mg II is good only to about a factor of 2. In addition, the Lα luminosities have to be considered a lower limit, since interstellar absorption does reduce the observed line strength.

VII. DISCUSSION

The UV and optical observations obtained during the 1976 campaign demonstrate that both HR 1099 and UX Ari contain components with highly active chromospheres. *Some* of the observed behavior could be interpreted as being due to circumstellar material, but *all* of the observations are consistent with a chromospheric model. The mean Lα and Mg II emission-line luminosity for both binaries is over 50 times that observed in the Sun's chromosphere (Tousey *et al.* 1974; McClintock *et al.* 1975). In addition, HR 1099 was found to exhibit exceptionally strong Ca II H and K and Hα emission. Although no optical spectroscopic observations of UX Ari were obtained, previous studies have also indicated this system exhibits strong emission in both spectral

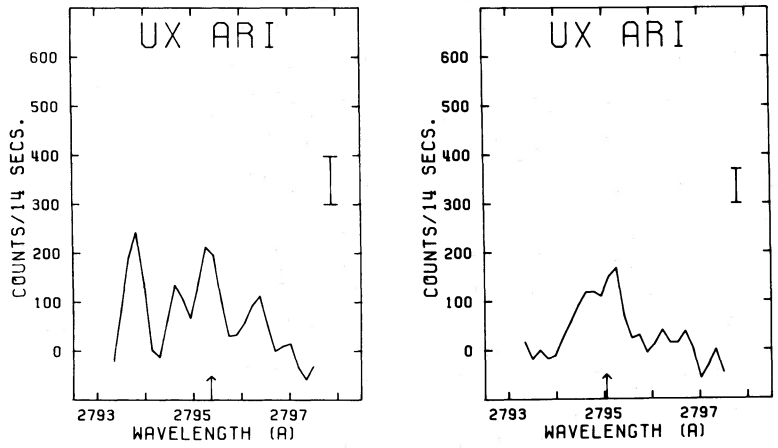

FIG. 13.—(*a*) Composite Mg II *k* line scan of UX Ari obtained over a 7 hr interval and centered at 0300 UT on October 2 around the time of the strong radio outburst. Note the strong feature near 2794 Å. The error bar is ±1 σ. Orbital phase is 0.55. (*b*) Composite Mg II *k* line scan of UX Ari obtained over a 6 hr interval and centered at 1400 UT on September 27. The error bar is ±1 σ. Orbital phase is 0.84.

TABLE 2

Lα AND Mg II EMISSION LUMINOSITY

LINE	LEVEL	LUMINOSITY HR 1099 (ergs s^{-1})	LUMINOSITY UX Ari (ergs s^{-1})
Lα.....	(highest)	9.8×10^{29}	9.1×10^{29}
Lα.....	(lowest)	5.0×10^{29}	4.7×10^{29}
Lα.....	(mean)	6.7×10^{29}	7.7×10^{29}
Mg II *k*.....	(highest)	1.8×10^{30}	2.0×10^{30}
Mg II *k*.....	(lowest)	6.1×10^{29}	9.7×10^{29}
Mg II *k*.....	(mean)	1.1×10^{30}	1.3×10^{30}
Mg II *h*.....	(highest)	2.0×10^{30}	...
Mg II *h*.....	(lowest)	6.8×10^{29}	...
Mg II *h*.....	(mean)	1.2×10^{30}	...

regions (Mulligan and Bopp 1975; Weiler 1978*a*). The source of both the UV and optical emission may be closely related to the surface or atmosphere of the more active star in each system, as the strongest emission features in all spectral regions were usually found to match the orbital velocity of this component.

Recent observations at McDonald Observatory support the surface phenomena concept in HR 1099. Barker and Polidan (1978) observed the λ8500 triplet of Ca II in HR 1099 over the course of several nights during late 1977. Their preliminary results indicate the variations seen in these emission lines and the narrowness of the line profiles are more compatible with surface activity than with disk or intrasystem material.

Further evidence for highly active chromospheres is provided by the observation of displaced Mg II emission lines from both binaries. These displaced features were present in about 75% of all composite Mg II profiles from both systems and may be caused by high-velocity gas motions similar in some sense to highly active prominences. These features on the Sun exhibit radial velocities of several hundred km s^{-1} (Severny 1959; Severny and Khokhlova 1953) and have lifetimes of several hours (Tandberg-Hanssen 1967). Assuming an electron density of about 10^{12} cm^{-3} and a temperature of about 8000 K (conditions typical of those found in solar-type prominences), Weiler (1978*b*) has calculated the total mass required to produce the displaced feature in Figure 12*b* to be about 10^{19} g (the mass of emitting Mg ions was 10^{10} g). This value is three orders of magnitude greater than the mass (10^{16} g) involved in active solar prominences (Kleczek 1964). The higher rotational velocity, stronger magnetic fields, and lower effective surface gravity expected on the more active star may combine to rationalize this large amount of material compared with solar values. Since the general activity level must be higher in these systems, as indicated by total line luminosity levels, we might expect all solar-type phenomena to be greatly enhanced. White, Sanford, and Weiler (1978) have recently reported an X-ray flare in the 2.5 to 7.5 keV range from HR 1099 coincident in time with the large radio flare on 1976 September 24 UT. In this regard we note the qualitative similarity of this and many of our observations to solar flarelike phenomena (e.g., Svetska 1976).

Alternate possibilities to consider for the source of the displaced Mg II emission lines are the less active star, intrasystem gas, or circumstellar gas. Weiler (1978*b*) has studied these sources on the grounds of the physical dimensions of the binary systems as well as the physical conditions necessary to produce the observed emission-line luminosity. He concluded that chromospheric gas motions or variable circumstellar ring or disk material are the most consistent explanation. Gas motions either produce the emission low in the chromosphere or at least supply material to form variable concentrations of emitting circumstellar gas. A stable disk was ruled out due to the lack of repeatability of displaced lines at similar orbital phases from HR 1099. This phenomenon could not be ruled out for UX Ari, however, as there was insufficient phase coverage.

Rhombs and Fix (1977) have detected a UV excess in three RS Canum Venaticorum systems, including UX Ari, which they interpreted as evidence for a hot circumstellar gas envelope, but their assumed gas temperature of 10^6 K is much too high to account for the displaced Mg II features. Naftilan and Drake (1977), however, recently have found marginal evidence for *variable* concentrations of circumstellar gas in the RS Canum Venaticorum binary AR Lacertae. Although the displaced Mg II emission features can be explained by this same phenomenon, we favor the first-order explanation of chromospheric gas motions in the lower atmosphere of the more active star. Since variable circumstellar material would probably be induced by variable surface activity, it seems unnecessary to postulate the former as the primary source of the emission. In addition, the coincident polarimetric observations indicate no evidence of variable polarization in either binary. Although this result does not completely rule out circumstellar material, it does place limits on the density, degree of ionization, and distribution of such material. The lack of variable polarization also suggests that large-scale mass transfer between the components is unlikely. Qualitatively, a mass concentration between the components would cause double-wave polarization curves over one orbital period. Polarization maxima should be observed near phase 0.25 and phase 0.75 where the scattering angles are the most favorable. No trace of such behavior can be seen from the polarimetric observations of either system (Figs. 3, 4). Admittedly, the polarization results are significant only if we are dealing with optically thin gas in the circumstellar or intrasystem regions. However, no dense mass streams between binary components or dense circumstellar gas have ever been observed in detached, late-type binary systems. (The components of HR 1099 fill only one-half of their Roche limiting surfaces [Weiler 1978*b*].) Moreover, electron densities in the radio emitting region are less than 10^{11} cm^{-3}, indicative of optically thin gas in the intrasystem region (see below). Thus it seems that the picture of

gas motions within the chromospheres of the more active component is the most consistent explanation of the Mg II observations.

In their model of active solar prominences, Jeffries and Orall (1965) assumed the resultant emission lines were optically thin. This assumption may be sound in the present case also, as it can explain the non-appearance of multiple velocity components in the coincident Ca II H and K observations. Calcium is about 20 times less abundant than magnesium (Allen 1963) and such features would be lost in the noise of the DDO data. In addition, a greater percentage of magnesium atoms will be in the singly ionized state throughout the chromosphere, since this species has a higher ionization potential than Ca II and will exist over a wider range of heights above the reversing layer. For these reasons, the Mg II doublet seems an excellent region to search for emission from chromospheric gas motions, especially since there is no continuum radiation to interfere with their visibility.

The higher-resolution Hα observations of HR 1099 from DDO also indicated the presence of multiple features. Stellar activity from the less active star can account easily for only one of these features in each observation. A visual comparison of the five nights of overlapping Mg II and Hα observations suggested a marginal similarity between the velocities of the displaced components in both spectral regions not attributable to the less active star. The Mg II observations indicated no evidence for an emission associated with the velocity of this star, but these data were too noisy to detect very weak features. The main emission line (presumably due to activity from the more active star) in both sets of observations also displayed marked profile variations which may be due to the intrinsic variation of the emission source, the effects of unresolved emission lines at various velocities, or a combination of both. More coordinated Hα and Mg II observations are planned to clarify the situation.

In addition to overall profile variations, the Hα line strength of HR 1099 from both Ritter and DDO observations was found to be variable. These variations were correlated to Lα emission behavior as shown in Figure 14. This figure is a plot of the normalized emission strength of Hα and Lα versus time and Julian date. The arrows along the abscissa represent successive photometric wave minima. Nightly mean measures of Hα emission EW are represented by D's (DDO) and H's (Ritter). Lα emission strengths are denoted by L's. There appears to be a good correlation between the Hα and Lα emission behavior. Furthermore, there may be some phase-rotation effect present, as maximum emission levels were observed on September 24 UT, near photometric wave minimum, while minimum emission was seen on October 1 UT, near wave maximum. The correlation of maximum emission intensity with photometric wave minimum has been observed for Ca II H and K and Hα in several other RS Canum Venaticorum systems (Bopp 1976; Mulligan and Bopp 1975; Weiler 1978*a*). Hall (1976) has suggested the distortion waves in RS Canum Venaticorum systems are

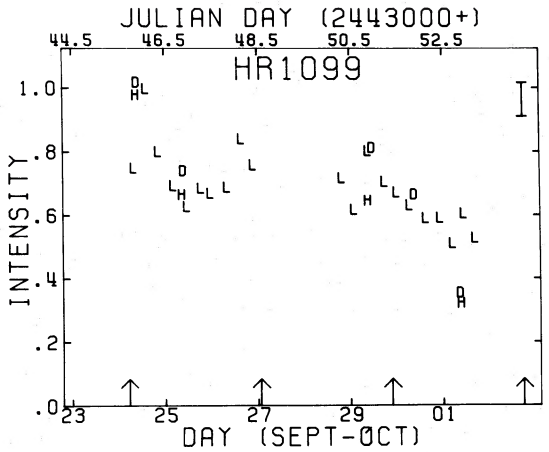

FIG. 14.—Normalized Hα and Lα emission intensity versus civil and Julian date for HR 1099. D's refer to Fraquelli's and H's to Bopp and Schmitz's nightly mean Hα equivalent widths. The L's represent the composite Lα emission intensity as determined by Weiler. The arrows along the abscissa refer to successive photometric wave minima, while the $\pm 1\,\sigma$ error bar for all observations appears at the upper right of the plot.

caused by extensive star spot activity on the surface of the cooler or subgiant components in these binaries. This interpretation is consistent with the results presented in Figure 14, but more data are required, over a longer time interval, to determine whether Hα and Lα emission are truly correlated with orbital phase and the photometric wave, or if some other effect can account for the marginal pattern seen in Figure 14.

The apparent agreement with a chromospheric model suggests that most of the observed emission occurs in a rather small volume close to the more active star in each system as compared with the radio activity. However, all of the observed emission may ultimately have the same energy source. Also, some of the observed emission-line activity may be related to the transport of energy into the larger volume within the binary system which probably contains the radio source.

Several arguments suggest that the radio emission occurs in a large volume. First, the lack of a cutoff in the radio spectrum implies that the plasma frequency is certainly less than 2695 MHz, therefore $n_e \lesssim 10^{11}\ \mathrm{cm}^{-3}$. This density is significantly lower than the 10^{12} to $10^{13}\ \mathrm{g\,cm}^{-3}$ which is likely for the Mg II emission features. Second, the circular polarization observed during this event indicates that if the emission process were magnetobremsstrahlung, the characteristic Lorentz factor of the electrons is certainly less than 10. This in turn implies a brightness temperature $\lesssim 10^{10}$ K and a size $\gtrsim 10^{11}$ cm in radius (Owen *et al.*). Third, the lack of an observable radio eclipse in a related system, AR Lac, also suggests a low brightness temperature and large size (Owen and Spangler 1977). Thus the source probably occupies a volume of much lower density and larger dimensions than the optical features.

While it seems clear that the radio emission is closely connected with the RS Canum Venaticorum phenomenon (e.g., Spangler *et al.*; Owen *et al.*), its relation to the surface phenomena observed in the optical and ultraviolet remains unclear. Three observations made during this campaign may suggest a direct correlation. First, the overall intensity levels of the Hα, Lα, and radio flux appear generally correlated during the September–October observations. In particular, the large radio flare from HR 1099 on September 24 UT occurred only a few hours earlier than the observations of maximum levels in both hydrogen emission lines. In addition, only at that time was short-term Hα flaring activity observed. Second, the flare observed at 1660 MHz at Jodrell Bank from UX Ari was coincident in time with the strongest Mg II multiple velocity emission feature observed from this system (Fig. 13*a*). Third, the strongest Mg II displaced feature observed from HR 1099 (Fig. 12*b*) corresponded in time with the rapid brightening at 2695 MHz on September 29 UT. However, it is not clear that these three coincidences alone provide conclusive evidence that the radio and visual–UV phenomena are causally related.

The observed Mg II gas may, however, be related to the transport and acceleration of the particles producing the radio emission. If we are watching a quasi-steady flow radially to or from the star, then the total energy, E_T, in the flow is

$$E_T = \frac{vt}{x}\frac{mv^2}{2},$$

where x is the scale height of the flaring region, v is the velocity of the flow, m is the mass of the ejected gas, and t is the characteristic lifetime of a large event. For $x \sim 10^3$ km, $v \sim 200$ km s^{-1}, $m \sim 10^{19}$ g, and $t \sim 4 \times 10^4$ s, then $E_T \sim 1.6 \times 10^{37}$ ergs, which is more than 10 times the minimum total energy implied by a large radio flare (Owen *et al.*). Thus, although the mechanism for producing the relativistic particles is not known, there appears to be enough energy in the mass motions to account for the radio source.

VIII. CONCLUSIONS

Multifrequency observations over the course of this campaign provide evidence for extensive and variable chromospheric activity on the cooler components of both HR 1099 and UX Ari. The radio emission probably occurs over a much larger volume than the visual and UV emission. Photometric observations indicate that both systems exhibit quasi-sinusoidal distortion waves with periods roughly equal to their orbital periods. Neither system displays significant broad-band visual polarization. At radio frequencies, however, HR 1099 is at times significantly circularly polarized. In HR 1099, Hα and Lα emission intensity appear to be temporally correlated and, in addition, they may also be correlated with the photometric distortion wave. Finally, there are suggestive coincidences between peak radio flux density and optical–UV emission activity from both systems. Further simultaneous observations are planned to clarify these points.

The authors would like to thank T. Jones for valuable discussions and T. Bolton and J. Percy for comments on the text. B. W. B. gratefully acknowledges support from NASA, the Research Corporation, and NSF grant AST 77 09450. E. J. W. gratefully acknowledges support from National Aeronautics and Space Administration contract NAS5-23576 with Princeton University. The authors are grateful to Mrs. Sue Hickey for her expert typing of the manuscript.

REFERENCES

Allen, C. W. 1963, *Astrophysical Quantities* (2d ed.; London: Athlone Press).
Anderson, R., and Weiler, E. J. 1978, *Ap. J.*, **224**, 143.
Barker, E. S., and Polidan, R. S. 1978, in preparation.
Bopp, B. W. 1976, *IAU Infor. Bull. Var. Stars*, No. 1175.
Bopp, B. W., and Fekel, F. 1976, *A.J.*, **81**, 771.
Bopp, B. W., Espenak, F., Hall, D. S., Landis, H. J., Lovell, L. P., and Reucroft, S. 1977, *A.J.*, **82**, 47.
Carlos, R. C., and Popper, D. M. 1971, *Pub. A.S.P.*, **83**, 504.
Gibson, D. M., Hjellming, R. M., and Owen, R. J. 1975, *Ap. J.* (*Letters*), **200**, L99.
Hall, D. S. 1972, *Pub. A.S.P.*, **84**, 323.
———. 1976, *IAU Colloquium No. 29, Multiple Periodic Variable Stars* (Dordrecht: Reidel), Part 1, p. 287.
———. 1977, *Acta Astr.*, **27**, 281.
Hine, J., and Ryle, M. 1978, in preparation.
Jeffries, J. T., and Orall, F. Q. 1965, *Ap. J.*, **141**, 505.
Kleczek, J. 1964, *Mass Balance in Flare Loops* (AAS–NASA Symposium on the Physics of Solar Flares).
Landis, H. J., Lovell, L. P., Hall, D. S., Henry, G. W., and Renner, T. 1978, *A.J.*, **83**, 176.
Latham, D. 1969, *AAS Photo Bull.*, **1**, 3.
McClintock, W. M., Linsky, J. L., Henry, R. C., Moos, H. W., and Gerola, H. 1975, *Ap. J.*, **202**, 165.
Mulligan, K., and Bopp, B. W. 1975, *IAU Infor. Bull. Var. Stars*, No. 1075.
Naftilan, S. A., and Drake, S. A. 1977, *Ap. J.*, **216**, 508.
Owen, F. N., and Gibson, D. M. 1978, in preparation.
Owen, F. N., Jones, T. W., and Gibson, D. M. 1976, *Ap. J.* (*Letters*), **210**, L27.
Owen, F. N., and Spangler, S. R. 1977, *Ap. J.* (*Letters*), **217**, L41.
Piirola, V. 1973, *Astr. Ap.*, **27**, 383.
———. 1975, *Ann. Acad. Sci. Fennicae*, Vol. **6**, No. 418.
Rhombs, C. G., and Fix, J. D. 1977, *Ap. J.*, **216**, 503.
Rogerson, J. B., Spitzer, L., Drake, J. F., Dressler, K., Jenkins, E. B., Morton, D. C., and York, D. G. 1973, *Ap. J.* (*Letters*), **181**, L97.
Severny, A. B. 1959, *Solar Physics* (Moscow: Foreign Language Publishing House).
Severny, A. B., and Khokhlova, V. L. 1953, *Iz. Krim. Ap. Obs.*, **10**, 9.
Snow, T. P., and Torres, C. M. 1977, *Copernicus Spectrometer Sensitivity III* (Princeton Univ. Obs. Memo to Users of *Copernicus* Data).
Spangler, S. R., Owen, F. N., and Hulse, R. A. 1977, *A.J.*, **82**, 989.
Svetska, Z. 1976, *Solar Flares* (Dordrecht: Reidel).

Tandberg-Hanssen, E. 1967, *Solar Activity* (Waltham, MA: Blaisdell).
Tousey, R., Milone, E. F., Purcell, J. D., Schneider, W., and Tilford, S. G. 1974, *An Atlas of the Solar Ultraviolet Spectrum between 2296 and 2992 Å* (NRL Rept., No. 7788).
Weiler, E. J. 1978*a*, *M.N.R.A.S.*, **182**, 77.
———. 1978*b*, *A.J.*, **83**, 795.
White, N. E., Sanford, P. W., and Weiler, E. J. 1978, *Nature*, in press.
Wilson, O. C. 1964, *Pub. A.S.P.*, **76**, 238.

BERNARD W. BOPP and MARION SCHMITZ: Department of Physics and Astronomy, University of Toledo, 2801 W. Bancroft St., Toledo, OH 43606

DOROTHY A. FRAQUELLI: David Dunlap Observatory, University of Toronto, Box 360, Richmond Hill, ON L4C 4Y6, Canada

DAVID M. GIBSON: Department of Physics and Astronomy, New Mexico Institute of Mining and Technology, Socorro, NM 87801

DOUGLAS S. HALL: Dyer Observatory, Vanderbilt University, Nashville, TN 37235

FRAZER N. OWEN: National Radio Astronomy Observatory, Edgemont Rd., Charlottesville, VA 22901

VILIPPU PIIROLA: University of Helsinki, Observatory and Astrophysics Laboratory, Tahtitorninmaki, SF-00130 Helsinki 13, Finland

MARTIN RYLE: Cavendish Laboratory, Madingley Rd., Cambridge CB3 0HE, England

EDWARD J. WEILER: Princeton University Observatory, Peyton Hall, Princeton, NJ 08540